Three Conformational Polymorphs of Di-μ-chlorotetrakis(1-methylboratabenzene)diyttrium: Synthesis, X-ray Structures, Quantum Chemical Calculations, and Lattice Energy Minimizations[1]

Xiaolai Zheng, Bing Wang, Ulli Englert, and Gerhard E. Herberich*

Institut für Anorganische Chemie, Technische Hochschule Aachen, Prof.-Pirlet-Strasse 1, D-52056 Aachen, Germany

Received December 27, 2000

The reaction of yttrium trichloride with lithium 1-methylboratabenzene (1/2) in toluene (110 °C, 3 days) afforded the donor-free dinuclear sandwich complex $[(C_5H_5BMe)_2Y(\mu\text{-Cl})]_2$ (**1**) in 85% yield as pale-yellow crystals. By means of single crystal and powder diffraction methods, three conformational polymorphs, α-**1** [$P2_1/n$ (No. 14), monoclinic, $a = 6.6124(8)$ Å, $b = 14.352(9)$ Å, $c = 14.120(1)$ Å, $\beta = 95.57(1)°$, $V = 1333.7(9)$ Å^3, $Z = 2$], β-**1** [$P2_1/a$ (No. 14), monoclinic, $a = 8.542(2)$ Å, $b = 13.712(6)$ Å, $c = 11.76(1)$ Å, $\beta = 102.60(4)°$, $V = 1344.5(13)$ Å^3, $Z = 2$], and γ-**1** [*Pbca* (No. 61), orthorhombic, $a = 20.091(5)$ Å, $b = 13.527(3)$ Å, $c = 9.976(2)$ Å, $V = 2711.2(11)$ Å^3, $Z = 4$], were characterized in the solid state of **1**. The molecules in the three phases vary remarkably in the rotational position of boratabenzene ligands with differences of 91.1, 133.1, and 24.9° between each pair. DFT calculations at the B3LYP/LanL2DZ level reveal that the three molecular structures observed in the solid state correspond closely to three minima on the gas-phase potential energy surface. The β conformation is 2.8 and 7.2 kJ/mol more stable than the α and γ conformations, respectively. Lattice energy minimizations predict that the α-**1** phase is about 5.5 and 18.7 kJ mol^{-1} more stable than the β-**1** and γ-**1** modifications, in agreement with the packing coefficients and the molecular volumes of the three crystal structures. While the α-**1** and β-**1** modifications have comparable total energies, the γ-**1** form is less stable. The total energy differences among the polymorphs are greater than generally expected.

Introduction

Polymorphism, the ability of a molecule to crystallize in more than one packing arrangement, is a rather popular chemical and crystallographic phenomenon.[2−4] A recent search in the Cambridge Structural Database (CSD) has shown that 5.5% of organometallic compounds are classified to be polymorphic whereas the percentage is only 4.1% for organic compounds.[5,6] However, the more frequently encountered organometallic polymorphism is much less investigated in comparison to the organic analogue. Because of some distinctive characteristics of organometallic species, such as metal−ligand delocalized bonding, fluxional behavior, and variable metallic oxidation states, understanding of this class of polymorphism cannot be achieved by simple extrapolation of the knowledge of the organic realm.[4,5]

Crystallization is indeed a molecular recognition process depending on subtle energetic equilibria concerning both intermolecular and intramolecular interactions.[7] While the lattice energy plays the predominant role in packing rigid molecules, the situation for molecules with soft internal degrees of freedom is more complicated. Polymorphism may occur as a result of arranging different conformations of the same molecule into different packing motifs with the additional possibility for each conformer to pack into several forms.

In our attempt to fully characterize the new boratabenzene complex di-μ-chlorotetrakis(1-methylboratabenzene)diyttrium (**1**) by conventional single crystal X-ray diffraction, we found that **1** crystallizes as concomitant polymorphs in $P2_1/n$ (α-**1**), $P2_1/a$ (β-**1**), and *Pbca* (γ-**1**) phases. The three modifications differ remarkably in the relative orientations of the boratabenzene ligands, displaying typical characteristics of conformational polymorphism. To avoid a pure enumeration of the resulting structural data and to achieve a better understanding of the energetic states of the polymorphs in terms of their molecular geometry and crystal packing, quantum chemical calculations and lattice energy minimizations were applied to rationalize the intra- and intermolecular interactions.

Computational Details

Quantum Chemical Calculations. All quantum chemical calculations were performed using the Gaussian 98 suite of programs.[8] The geometries were optimized with the help of density functional theory (DFT);[9] the Becke's three-parameter hybrid exchange functional[10] with

(1) Borabenzene Derivatives. 34. Part 33: Zheng, X.; Herberich, G. E. *Organometallics* **2000**, *19*, 3751.

(2) (a) McCrone, W. C. In *Physics and Chemistry in the Organic State*; Fox, D., Labes, M. M., Weissberger, A. Eds.; Interscience: New York, 1965; Vol. 2, p 726. (b) Byrn, S. R. In *Solid State Chemistry of Drugs*; Academic Press: New York, 1982; p 79. (c) Bernstein, J. In *Organic Solid State Chemistry*; Desiraju, G. R. Ed.; Elsevier: Amsterdam, 1987; p 471. (d) DeCamp, W. H. In *Crystal Growth of Organic Materials*; Myerson, A. S., Green, D. A., Meenan, P., Eds.; American Chemical Society: Washington, DC, 1996; p 66.

(3) (a) Dunitz, J.; Bernstein, J. *Acc. Chem. Res.* **1995**, *28*, 193. (b) Dunitz, J. *Acta Crystallogr. B* **1995**, *51*, 619. (c) Threlfall, T. L. *Analyst* **1995**, *120*, 2435.

(4) (a) Braga, D.; Grepioni, F. *J. Chem. Soc., Chem. Commun.* **1996**, 571. (b) Braga, D.; Grepioni, F. *Acc. Chem. Res.* **1994**, *27*, 51.

(5) Braga, D.; Grepioni, F. *Chem. Soc. Rev.* **2000**, *29*, 229; the CSD search was carried out in March 2000.

(6) A previous CSD search in 1983 showed that 5% of structurally characterized compounds were classified to be polymorphic. See: Allen, F. H.; Kennard, O.; Taylor, R. *Acc. Chem. Res.* **1983**, *16*, 146.

(7) (a) Dunitz, J. D. *Pure Appl. Chem.* **1991**, *63*, 177. (b) Buttar, D.; Charlton, M. H.; Docherty, R.; Starbuck, J. *J. Chem. Soc., Perkin Trans. 2* **1998**, 763.

10.1021/ic0014641 CCC: $20.00
Published on Web 05/19/2001

Table 1. Interaction Parameters for the van der Waals Potential[a]

atom−atom interaction	potential code	A, kJ mol^{-1} Å^{-6}	B, kJ mol^{-1}	C, Å^{-1}	r_0, Å	$r_{min,}$ Å	$E_{min,}$ kJ mol^{-1}	$\lambda = Cr_{min}$
H···H	P1, P2	144.2	11 104	3.74	2.831	3.229	−0.064	12.08
C···C, B···B	P1, P2	2377	349 908	3.60	3.451	3.882	−0.396	13.98
Cl···Cl	P1, P2	6000	1 000 000	3.56	3.592	4.032	−0.813	14.35
Y···Y	P1	6463	1 804 000	4.00	3.110	3.498	−2.016	14.00
Y···Y	P2	12 000	1 500 000	3.36	3.839	4.306	−1.102	14.47

[a] r_0 = distance where $E = 0$; r_{min} = minimum of the potential curve; E_{min} = depth of the potential curve; λ = steepness of the potential curve; interaction parameters between different atoms were calculated according to the combining rules.

nonlocal correction potentials of Lee, Yang, and Parr[11] (B3LYP) was applied. In addition, the gas-phase electronic energies at the Hartree−Fock (HF) and the second-order Møller−Plesset perturbation (MP2)[12] levels were computed by single point calculations on the basis of the DFT geometries.

The Dunning/Huzinaga all-electron basis sets[13] with double-ξ quality were used to describe hydrogen and the first-row atoms; the yttrium atom was approximated by the basis set of Hay and Wadt.[14] The description of the valence electrons was of double-ξ quality whereas the core electrons were replaced by quasirelativistic effective core potentials (ECP). The so-defined basis set LanL2DZ was employed throughout our computations.

Lattice Energy Minimizations. Lattice energy minimizations were performed using the PCK 83 program.[15] Intermolecular van der Waals (vdW) forces were computed with the help of the atom−atom potential method using Buckingham potentials (eq 1) in which r_{ij} represents the interatomic distance and A, B, and C are empirical interaction parameters.[16,17] The molecules were treated as rigid bodies; the atomic coordinates were taken from the corresponding single crystal structures with all C−H bond lengths being modified to a more reasonable value of 1.05 Å. Forces other than vdW forces were neglected in view of a largely unpolar periphery of the molecules involved.

$$E_{vdW} = {}^1/_2 \sum_i \sum_j -Ar_{ij}^{-6} + Be^{-Cr_{ij}} \quad (1)$$

The interaction parameters used in our minimizations are summarized in Table 1. The parameters for carbon and hydrogen were published by Williams,[16b] and we used carbon parameters to describe the boron atom. In general, no reliable vdW descriptors are available for atoms such as rare earth metals that cannot reside in the molecular periphery. We chose parameters for yttrium on the basis of general expectations for larger atoms with more electrons and used two different sets P1 and P2 to judge the influence of parametrization on the result of the calculations. A similar procedure had been utilized successfully in our earlier work.[17] The interaction parameters between different atoms were generated according to the following combining rules: $A_{12} = (A_{11} \times A_{22})^{1/2}$, $B_{12} = (B_{11} \times B_{22})^{1/2}$, and $C_{12} = (C_{11} + C_{22})/2$.[16,17]

Packing Coefficient Calculations. The packing coefficient of each polymorphic modification was evaluated according to Gavezzotti's sampling method.[18] The following vdW radii were used: Y 2.10, Cl 1.77, C 1.75, B 1.70, and H 1.17 Å.

Results and Discussion

Synthesis. Boratabenzene anions are six-membered aromatic heterocycles which can serve as 6π electron ligands.[19] While intensive previous work has been dedicated to the boratabenzene complexes of late transition metals, complexes of scandium, a rare earth metal, appeared only very recently.[20] We report here the synthesis of $[(C_5H_5BMe)_2Y(\mu\text{-Cl})]_2$, the first boratabenzene complex of yttrium.

Treatment of yttrium trichloride with 2 equiv of lithium 1-methylboratabenzene[21] afforded the donor-free yttrium sandwich complex **1** in 85% yield as moisture sensitive pale yellow crystals (eq 2).

$$4Li(C_5H_5BMe) + 2YCl_3 \rightarrow \underset{\mathbf{1}}{[(C_5H_5BMe)_2Y(\mu\text{-Cl})]_2} + 4LiCl \quad (2)$$

The reaction was carried out using toluene as the solvent. Because of the lower nucleophilicity of $Li(C_5H_5BMe)$ in comparison to cyclopentadienide,[22] relatively severe reaction conditions (110 °C, 3 days) were required to complete the reaction. Compound **1** was characterized by mass spectroscopy,

(8) Frisch, M. J.; Trucks, G. W.; Schlegel, H. B.; Scuseria, G. E.; Robb, M. A.; Cheeseman, J. R.; Zakrzewski, V. G.; Montgomery, J. A., Jr.; Stratmann, R. E.; Burant, J. C.; Dapprich, S.; Millam, J. M.; Daniels, A. D.; Kudin, K. N.; Strain, M. C.; Farkas, O.; Tomasi, J.; Barone, V.; Cossi, M.; Cammi, R.; Mennucci, B.; Pomelli, C.; Adamo, C.; Clifford, S.; Ochterski, J.; Petersson, G. A.; Ayala, P. Y.; Cui, Q.; Morokuma, K.; Malick, D. K.; Rabuck, A. D.; Raghavachari, K.; Foresman, J. B.; Cioslowski, J.; Ortiz, J. V.; Stefanov, B. B.; Liu, G.; Liashenko, A.; Piskorz, P.; Komaromi, I.; Gomperts, R.; Martin, R. L.; Fox, D. J.; Keith, T.; Al-Laham, M. A.; Peng, C. Y.; Nanayakkara, A.; Gonzalez, C.; Challacombe, M.; Gill, P. M. W.; Johnson, B. G.; Chen, W.; Wong, M. W.; Andres, J. L.; Head-Gordon, M.; Replogle, E. S.; Pople, J. A. *Gaussian 98*, revision A.7; Gaussian, Inc.: Pittsburgh, PA, 1998.

(9) (a) Kohn, W.; Sham, L. J. *Phys. Rev.* **1965**, *140*, 1133. (b) Parr, R. G.; Yang, W. *Density Functional Theory of Atoms and Molecules*; Oxford University Press: Oxford, 1989. (c) Perdew, J. P.; Chevary, J. A.; Vosko, S. H.; Jeckson, K.; Pederson, M. R.; Singh, D. J.; Fiolhais, C. *Phys. Rev. B* **1992**, *46*, 6671. (d) Laird, B. B., Ross, R. B., Ziegler, T., Eds. *Chemical Applications of Density Functional Theory*; ACS Symp. Ser. 629; American Chemical Society: Washington, DC, 1996.

(10) (a) Becke, A. D. *Phys. Rev. A* **1988**, *88*, 563. (b) Becke, A. D. *J. Chem. Phys.* **1992**, *96*, 2155. (c) Becke, A. D. *J. Chem. Phys.* **1993**, *98*, 1372. (d) Becke, A. D. *J. Chem. Phys.* **1993**, *98*, 5648.

(11) (a) Lee, C.; Yang, W.; Parr, R. G. *Phys. Rev. B* **1988**, *37*, 785. (b) Miehlich, B.; Savin, A.; Stoll, H.; Preuss, H. *Chem. Phys. Lett.* **1989**, *157*, 200.

(12) (a) Head-Gordon, M.; Pople, J. A.; Frisch, M. J. *Chem. Phys. Lett.* **1988**, *153*, 503. (b) Frisch, M. J.; Head-Gordon, M.; Pople, J. A. *Chem. Phys. Lett.* **1990**, *166*, 275. (c) Frisch, M. J.; Head-Gordon, M.; Pople, J. A. *Chem. Phys. Lett.* **1990**, *166*, 287.

(13) Dunning, T. H., Jr; Hay, P. J. In *Modern Theoretical Chemistry*; Schaefer, H. F., III, Ed.; Plenum: New York, 1976; Vol. 3, p 1.

(14) (a) Hay, P. J.; Wadt, W. R. *J. Chem. Phys.* **1985**, *82*, 270. (b) Wadt, W. R.; Hay, P. J. *J. Chem. Phys.* **1985**, *82*, 284. (c) Hay, P. J.; Wadt, W. R. *J. Chem. Phys.* **1985**, *82*, 299.

(15) Williams, D. E. *PCK83 - A Crystal Molecular Packing Analysis Program*; Quantum Chemistry Programs Exchange, 1983.

(16) (a) Pertsin, A. J.; Kitaigorodsky, A. I. *The Atom-Atom Potential Method*; Springer: Berlin, 1986. (b) Williams, D. E. *J. Chem. Phys.* **1967**, *47*, 4680.

(17) (a) Englert, U. In *Advances in Molecular Structure Research*; Hargittai, M., Hargittai, I., Eds.; JAI Press Inc.: Greenwich, CT, 2000; Vol. 6, p 49. (b) Schmidt, M. U.; Englert, U. *J. Chem. Soc., Dalton Trans.* **1996**, 2077.

(18) Gavezzotti, A. *J. Am. Chem. Soc.* **1983**, *105*, 5220.

(19) (a) Herberich, G. E.; Ohst, H. *Adv. Organomet. Chem.* **1986**, *25*, 119. (b) Herberich, G. E. Boratabezene chemistry revisited. In *Advances in Boron Chemistry*; Siebert, W., Ed.; The Royal Society of Chemistry: Cambridge, U.K., 1997. Special Publication No. 201, p 211. (c) Ashe, A. J., III.; Al-Ahmad, S.; Fang, X. *J. Organomet. Chem.* **1999**, *581*, 92.

(20) (a) Putzer, M. A.; Rogers, J. S.; Bazan, G. C. *J. Am. Chem. Soc.* **1999**, *121*, 8112. (b) Herberich, G. E.; Englert, U.; Fischer, A.; Ni, J.; Schmitz, A. *Organometallics* **1999**, *18*, 5496.

(21) Herberich, G. E.; Schmidt, B.; Englert, U. *Organometallics* **1995**, *14*, 471.

(22) Herberich, G. E.; Rosenplänter, J.; Schmidt, B.; Englert, U. *Organometallics* **1997**, *16*, 926.

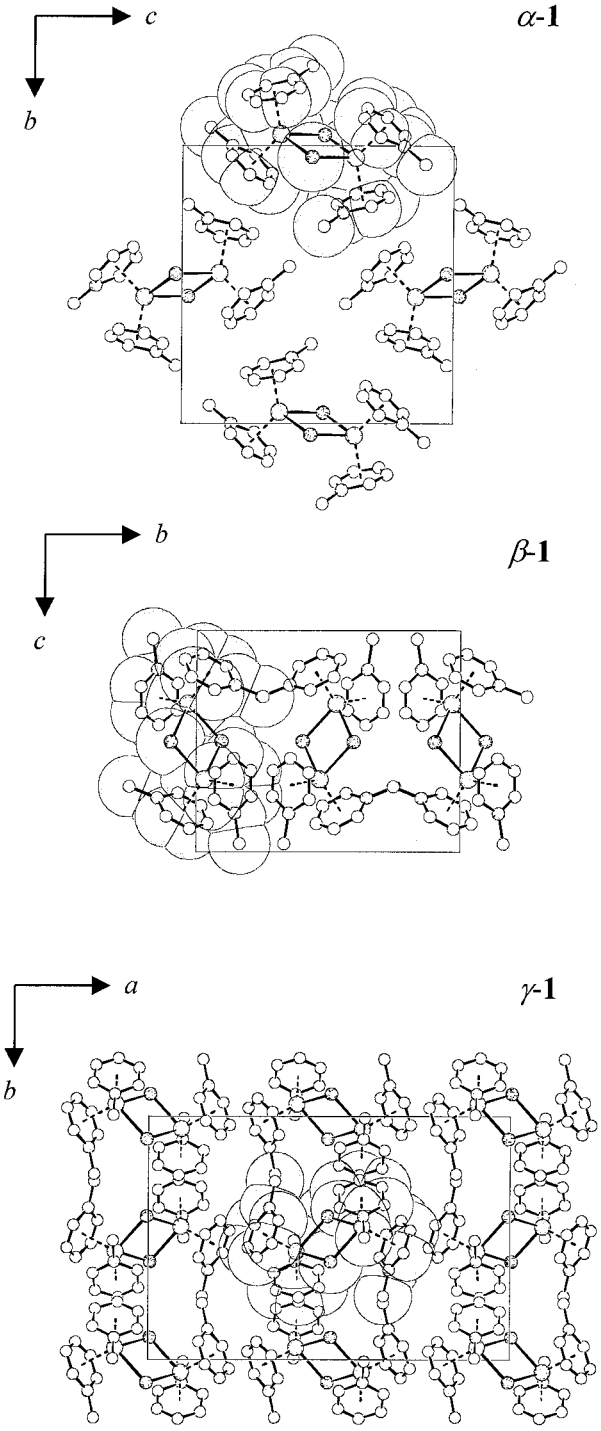

Figure 1. Packing diagrams of α-**1**, *β*-**1**, and *γ*-**1** phases (SCHAKAL[23]). Hydrogen atoms are omitted for clarity.

multinuclear NMR spectroscopy, elemental analysis, and single crystal and powder diffraction.

X-ray Diffraction Studies. Three crystal phases, namely, $P2_1/n$ (α-**1**), $P2_1/a$ (*β*-**1**), and *Pbca* (*γ*-**1**), were encountered in the solid state of **1** when single crystals were picked and subjected to X-ray diffraction (Figures 1 and 2, Table 2). Note that no valid lattice transformation exists between the two monoclinic structures of α-**1** and *β*-**1**, which belong to the same space group (No. 14). All crystals have the same light yellow color; the crystals of the α-**1** and *γ*-**1** forms turn out to be more anisotropic and rod-shaped. The intensity data sets of the three modifications were first collected at 20 °C. Refinement showed that the room-temperature data set of *γ*-**1** was of moderate

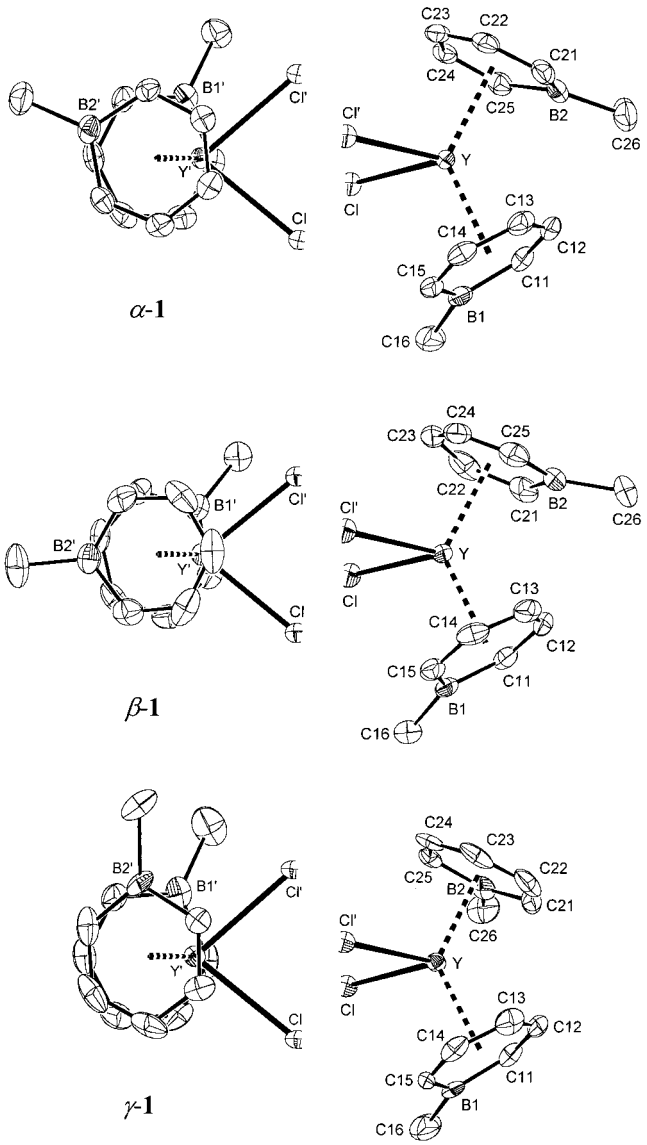

Figure 2. Simplified top and side views of the molecular structures of α-**1**, *β*-**1**, and *γ*-**1** phases showing the variable orientations of boratabenzene ligands (PLATON[24]). The two columns present different halves of the molecules which are related to each other with a crystallographic inversion center. Displacement ellipsoids are scaled to the 30% probability level.

quality. An additional data set from the same crystal at −60 °C gave better agreement factors and smaller estimated standard deviations. Hence, the geometry of this low-temperature structure is documented in this section together with the other two forms.

Several common features are shared by these polymorphic modifications. First, all three structures display dinuclear molecules: Two bent sandwich units are connected by two bridging chlorine atoms with respect to a crystallographic inversion center. This type of structure is quite common for lanthanide(III) sandwich complexes[25] and has been documented, for example, for $[(C_5H_5)_2Sc(\mu\text{-}Cl)]_2$,[26a] $[(MeC_5H_4)_2Yb(\mu\text{-}Cl)]_2$,[26b] and $[(Me_3SiC_5H_4)_2Y(\mu\text{-}Cl)]_2$[26c] as well as for the boratabenzene compound $[(C_5H_5BMe)_2Sc(\mu\text{-}Cl)]_2$.[20b] Second, the geometries of the Y_2Cl_2 cores are similar among the three phases. Only

(23) Keller, E. *SCHAKAL88 - A FORTRAN Program for the Graphic Representation of Molecular and Crystallographic Models*; University of Freiburg: Freiburg, Germany, 1988.
(24) Spek, A. L. *Acta Crystallogr. A* **1990**, *46*, C34.

Table 2. A Comparison of Geometrical Parameters for α-**1**, *β*-**1**, and *γ*-**1**[a]

	α-**1**		*β*-**1**		*γ*-**1**	
	exptl	calcd	exptl	calcd	exptl	calcd
Y−Cl, Å	2.6733(6)	2.774	2.680(2)	2.785	2.661(1)	2.766
Y−Cl′, Å	2.6844(7)	2.778	2.693(2)	2.780	2.684(2)	2.781
Cl−Y−Cl′, deg	80.66(2)	78.83	78.90(5)	78.43	80.52(5)	78.55
Y−Bb1, Å	2.335	2.386	2.337	2.389	2.336	2.390
Y−Bb2, Å	2.328	2.384	2.345	2.377	2.325	2.383
Bb1−Y−Bb2, deg	129.9	131.0	129.3	129.6	127.6	128.6
τ_1, deg	63.8	65.1	52.7	47.7	65.4	70.2
τ_2, deg	154.9	157.6	185.8	182.8	90.3	93.4
$\Delta\tau$, deg	91.1	92.5	133.1	135.2	24.9	23.2

[a] τ_1 and τ_2: the angles between the Y···Y′ vector and the projections of the exocyclic B1−C16 (τ_1) and B2−C26 (τ_2) bond vectors onto the equatorial Y_2Cl_2 plane. $\Delta\tau = \tau_2 - \tau_1$. Y−Bb1 and Y−Bb2: the distances of the metal to the best C_5B planes (Bb1 C11−C15, B1; Bb2 C21−C25, B2). Bb1−Y−Bb2: the bending angles of sandwich units.

small variations are observed in the average Y−Cl bond distances (2.673−2.687 Å) and Cl−Y−Cl′ angles (78.90−80.66°). Finally, all boratabenzene C_5B rings are approximately planar with the boron atoms slightly bending away from the metal.[27,28] The average Y−C bond lengths (α-**1**, 2.706 Å; *β*-**1**, 2.707 Å; *γ*-**1**, 2.706 Å) are virtually identical for the three phases and are significantly longer than those in $[(Me_3SiC_5H_4)_2Y(\mu\text{-}Cl)]_2$ (2.628 Å).[26c] This observation is in agreement with the relatively poor electron donor quality of the 1-methylboratabenzene ligand.[22] We note that the similarity in bond distances and angles among different modifications is a common aspect of conformational polymorphism. This is due to the fact that the crystal field cannot account for the relatively high energies required to distort these parameters.[7,29]

However, the α-**1**, *β*-**1**, and *γ*-**1** phases differ dramatically in both molecular shapes and packing motifs. At the crystal level, the molecular arrangements are completely different (Figure 1). In absence of other significant intermolecular interactions, all three structures can be regarded as vdW assemblies. The *γ*-**1** structure possesses the highest variation in its packing density; it exhibits relatively shorter intermolecular interactions (H···H of ca. 2.25 Å) as well as larger voids among the neighboring molecules.

At the molecular level, while one boratabenzene ring (B1, C11−C16) of the three structures displays a rotational position ensuring a reasonable methyl···chlorine contact (C16···Cl = 3.6−3.7 Å), the relative orientations of the second boratabenzene ligand turn out to be quite different (Figure 2). We defined two parameters, τ_1 and τ_2, as the angles between the Y···Y′ vector and the projections of exocyclic B1−C16 (τ_1) or B2−C26 (τ_2) bond vectors onto the equatorial Y_2Cl_2 plane to describe the rotational positions of the ligands. The difference between τ_1 and τ_2, $\Delta\tau$, therefore corresponds to the torsional angle between the boratabenzene ligands of a bent sandwich moiety. Highly variable $\Delta\tau$ values, 91.1° in α-**1**, 133.1° in *β*-**1**, and 24.9° in *γ*-**1**, are encountered, revealing that the present phenomenon is in fact a typical conformational polymorphism[5] arising from the rotational flexibility of facially bonded *π*-ligands. Despite the marked variability of the $\Delta\tau$'s, the relative orientations between the boratabenzene ligands are not arbitrary: The three polymorphic conformations represent three different intramolecular arrangements to interlock the substantially sizable boratabenzene rings in energetically favorable ways. CPK representations of the three molecules are available in the Supporting Information.

A powder diffraction experiment for one crop of ground crystals was performed at ambient temperature. The diffraction pattern within a well-resolved 2θ range (7−16°) was simulated against the single crystal structures (Figure 3). All lines can be assigned on the basis of the three known phases which rules out the existence of any additional crystalline form under our experimental conditions. The simulation results show that the sample is composed of ca. 80% of α-**1**, 10% of *β*-**1**, and 10% of *γ*-**1**. Not too much importance should be attributed to these absolute values, because for concomitant polymorphs[30] the composition may vary depending on the crystallization conditions.

In the solid state of ferrocene[31,32] the existence of three temperature-dependent crystalline modifications, i.e., one ambient temperature disordered and two low temperature ordered phases, is well documented. The molecular shapes present in the ferrocene modifications are staggered, eclipsed, and intermediate with torsional angles of 36, 0, and 9°, respectively. In comparison, the three polymorphs of compound **1** were obtained from the same crystallization process. They are all well-ordered and stable at room temperature. Why can these three phases coexist in the solid state? To discuss this question, we recurred to theoretical gas-phase electronic energy calculations and empirical force-field lattice energy minimizations.

Quantum Chemical Calculations. Density functional theory has recently found intensive applications in theoretical chemistry

(25) (a) Edelmann, F. T. In *Metallocenes*; Togni, A., Halterman, R. L., Eds.; Wiley-VCH: Weinheim, Germany, 1998; Vol. 1, p 55. (b) Chirik, P. J.; Bercaw, J. E. In *Metallocenes*; Togni, A., Halterman, R. L., Eds.; Wiley-VCH: Weinheim, Germany, 1998; Vol. 1, p 111. (c) Bombieri, G.; Paolucci, G. In *Handbook on the Physics and Chemistry of Rare Earths*; Gschneidner, K. A., Jr., Eyring, L., Eds.; Elsevier Science: Amsterdam, The Netherlands, 1998; Vol. 25, p 265. (d) Schumann, H.; Meese-Marktscheffel, J. A.; Esser, L. *Chem. Rev.* **1995**, *95*, 865.

(26) (a) Atwood, J. L.; Smith, K. D. *J. Chem. Soc., Dalton Trans.* **1973**, 2487. (b) Baker, E. C.; Brown, L. D.; Raymond, K. N. *Inorg. Chem.* **1975**, *14*, 1376. (c) Evans, W. J.; Sollberger, M. S.; Shreeve, J. L.; Olofson, J. M.; Hain, J. H., Jr.; Ziller, J. W. *Inorg. Chem.* **1992**, *31*, 2492.

(27) (a) Zheng, X.; Englert, U.; Herberich, G. E.; Rosenplänter, J. *Inorg. Chem.* **2000**, *39*, 5579. (b) Herberich, G. E.; Englert, U.; Schmitz, A. *Organometallics* **1997**, *16*, 3751.

(28) Bazan, G. C.; Rodriguez, G.; Ashe, A. J., III; Al-Ahmad, S.; Müller, C. *J. Am. Chem. Soc.* **1996**, *118*, 2291.

(29) (a) Wolff, J. J. *Angew. Chem., Int. Ed. Engl.* **1996**, *35*, 2195. (b) Bernstein, J.; Hagler, A. T. *J. Am. Chem. Soc.* **1978**, *100*, 673.

(30) Bernstein, J.; Davey, R. J.; Henck, J.-O. *Angew. Chem., Int. Ed.* **1999**, *38*, 3440.

(31) (a) Braga, D. *Chem. Rev.* **1992**, *92*, 369. (b) Dunitz, J. D. In *Organic Chemistry: Its Language and its State of the Art*; Kisakürek, M. V., Ed.; Verlag HCA: Basel, 1993; p 9.

(32) (a) Clec'h, G.; Calvarin, G.; Berar, J. F.; Kahn, R. *Acad. Sci. Ser. C* **1978**, *286*, 315. (b) Seiler, P.; Dunitz, J. D. *Acta Crystallogr. B* **1979**, *35*, 1068. (c) Takusagawa, F.; Koetzle, T. F. *Acta Crystallogr. B* **1979**, *35*, 1074. (d) Seiler, P.; Dunitz, J. D. *Acta Crystallogr. B* **1979**, *35*, 2020. (e) Ogasahara, K.; Sorai, M.; Suga, H. *Chem. Phys. Lett.* **1979**, *68*, 457. (f) Seiler, P.; Dunitz, J. D. *Acta Crystallogr. B* **1982**, *38*, 1741. (g) Braga, D.; Grepioni, F. *Organometallics* **1992**, *11*, 711.

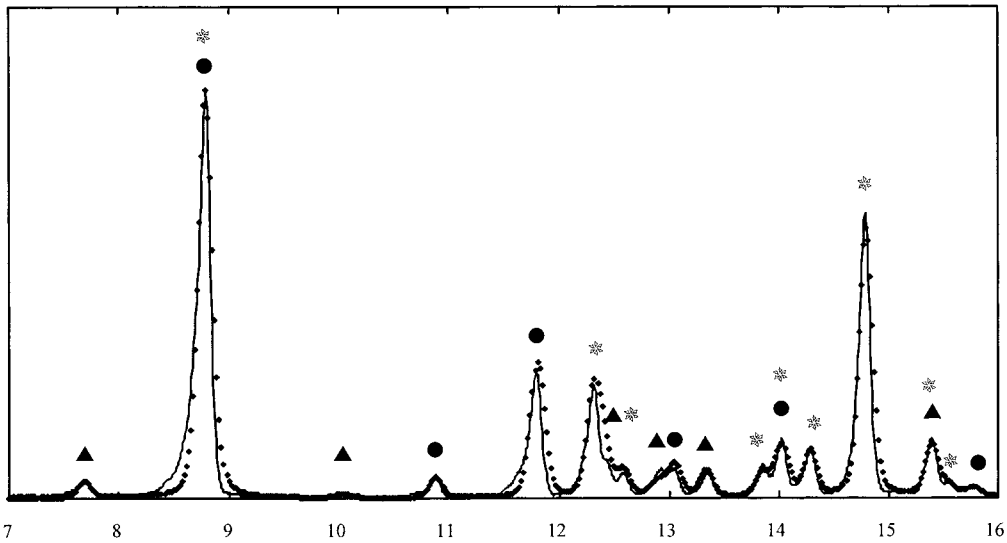

Figure 3. Experimentally observed (solid line) and simulated (dotted line) powder patterns (relative intensity vs diffraction angle 2θ) for **1**. The contributions of individual polymorphs are marked with * (α-**1**), ▲ (β-**1**), and ● (γ-**1**).

Table 3. Calculated Gas-Phase Electronic Energies for α-**1**, β-**1**, and γ-**1**

	α-**1**	β-**1**	γ-**1**
	B3LYP/LanL2DZ		
E_{el}, au	−1139.36318	−1139.36426	−1139.36151
ΔE_{el}, kJ mol^{-1}	2.8	0	7.2
	HF//B3LYP/LanL2DZ		
E_{el}, au	−1130.86312	−1130.86342	−1130.86082
ΔE_{el}, kJ mol^{-1}	0.8	0	6.8
	MP2//B3LYP/LanL2DZ		
E_{el}, au	−1133.47987	−1133.48151	−1133.48429
ΔE_{el}, kJ mol^{-1}	4.3	0	7.3

because it provides reliable electronic structures for a wide variety of compounds.[33] Taking the X-ray structures as the starting points, the molecular geometries present in the three modifications were optimized at the B3LYP/LanL2DZ level under a constrain of C_i point group symmetry. The computed geometrical parameters are compared to the corresponding data from the single crystal diffraction work and generally show good agreement (Table 2). The calculated torsional positions of boratabenzene rings are $\Delta\tau$(α-**1**) = 92.5°, $\Delta\tau$(β-**1**) = 135.1°, and $\Delta\tau$(γ-**1**) = 23.2°. These values reproduce the experimental results quite well. Thus, the three crystalline modifications correspond closely to three minima on the gas-phase potential energy surface.

The computed absolute and relative electronic energies (E_{el} and ΔE_{el}) are summarized in Table 3. Within the framework of the DFT calculations, the β-**1** conformation is 2.8 and 7.2 kJ/mol more stable than the α-**1** and γ-**1** forms, respectively. For the sake of comparison, single point calculations at the HF and the MP2 levels were also performed on the DFT-optimized geometries using the same basis set; both methods reproduce the stability sequence, β-**1** < α-**1** < γ-**1**, with only small differences in ΔE_{el}. Because of the fairly large size of **1** as well as the complicated relative positions of the boratabenzene ligands, we were unable to compute rotational barriers by investigating the potential energy surface. The relatively small ΔE_{el} values suggest that crystal field effects could override this sequence.

Lattice Energy Minimizations. Force-field type lattice energy calculations based on the atom−atom potential method[16,17] were applied to analyze the effect of packing energies on the present polymorphism (Table 4). Two sets of interaction parameters, denoted as P1 and P2, with different yttrium parameters, were used in our calculations. To exclude the influence of the temperature on the lattice energy calculations,[32g] the minimizations were performed starting from the room-temperature structures.

In all three cases, the optimized structural motifs reproduce the packing arrangements determined by the X-ray diffraction method. The experimental lattice constants are underestimated by about 2−4% and the cell volumes by about 6−8%. This conforms to general observations and is caused by the fact that the atom−atom potential based lattice energy minimizations reproduce structures at 0 K.[34] The computational results show that parameter set P1 gives slightly higher absolute lattice energies (E_{latt}) than P2. However, the relative lattice energies (ΔE_{latt}) are comparable between the two sets. The insensitivity of ΔE_{latt} to the yttrium potential parameters can obviously be related to the absence of significant short-distance vdW interactions between the metal and atoms from the neighboring molecules.

Our calculations give the lattice energy order α-**1** < β-**1** < γ-**1** for the three polymorphs, and the α-**1** form is 5.5 and 18.7 kJ mol^{-1} (av) more stable than β-**1** and γ-**1**, respectively. We note that the same sequence is suggested by the molecular volumes (V/Z) and packing coefficients (α-**1**, 71.0%; β-**1**, 69.3%; γ-**1**, 67.6%). In the absence of other specific intermolecular interactions such as hydrogen bonds, the V/Z values or densities represent the packing efficiency and hence can give a hint as to lattice energy relationships.[35]

Total Energies. It is generally accepted that polymorphism should be understood in terms of total energy, taking into account both intramolecular and intermolecular interactions.[7] The conformational isomers correspond to different energy minima along the interconversion pathway. Therefore, thermodynamically less stable isomers may be isolated in the solid state if the enthalpy difference between the free molecules is compensated by a gain in lattice energy.[2−5] The relationship between the α-**1** and β-**1** phases is in line with this discussion. The slightly more favorable crystal packing of the α-**1** form

(33) (a) Ziegler, T. *Chem. Rev.* **1991**, *91*, 651. (b) Niu, S. Hall, B. *Chem. Rev.* **2000**, *100*, 353.

(34) Gavezzotti, A.; Filippini, G. *J. Chem. Soc., Chem. Commun.* **1998**, 287.

(35) Gavezzotti, A.; Filippini, G. *J. Am. Chem. Soc.* **1995**, *117*, 12299.

Table 4. Lattice Energy Minimizations of α-**1**, *β*-**1**, and *γ*-**1**

		a, Å	*b*, Å	*c*, Å	*β*, deg	*V*, Å^3	*V*/*Z* , Å^3	E_{latt}, kJ mol^{-1}	ΔE_{latt}, kJ mol^{-1}
α-**1**	exptl	6.6124(8)	14.352(9)	14.120(1)	95.57(1)	1333.7(9)	666.8		
	min/P1	6.325	14.206	13.713	94.48	1228.5	614.3	−186.9	0
	min/P2	6.329	14.196	13.703	94.46	1227.4	613.7	−192.3	0
β-**1**	exptl	8.542(2)	13.712(6)	11.76(1)	102.60(4)	1344.5(13)	672.2		
	min/P1	8.267	13.311	11.654	103.77	1245.5	622.8	−181.2	5.7
	min/P2	8.257	13.304	11.647	103.75	1242.8	621.4	−187.1	5.2
γ-**1**	exptl	20.293(4)	13.559(2)	10.014(3)		2755.4(11)	688.8		
	min/P1	19.634	13.274	9.899		2579.5	643.9	−168.1	18.8
	min/P2	19.618	13.259	9.891		2572.9	643.2	−173.7	18.6

Table 5. Crystal Data, Data Collection Parameters, and Convergence Results for α-**1**, *β*-**1**, and *γ*-**1**

	α-**1**	*β*-**1**	*γ*-**1**	
chem form.	$C_{24}H_{32}B_4Cl_2Y_2$	$C_{24}H_{32}B_4Cl_2Y_2$	$C_{24}H_{32}B_4Cl_2Y_2$	
fw	612.48	612.48	612.48	
λ, Å	0.7107	0.5609	0.7107	
space group	$P2_1/n$ (No. 14)	$P2_1/a$ (No. 14)	*Pbca* (No. 61)	
Z	2	2	4	
a, Å	6.6124(8)	8.542(2)	20.293(4)	20.091(5)
b, Å	14.352(9)	13.712(6)	13.559(2)	13.527(3)
c, Å	14.120(1)	11.76(1)	10.014(3)	9.976(2)
β, deg	95.57(1)	102.60(4)		
V, Å^3	1333.7(9)	1344.5(13)	2755.4(11)	2711.2(11)
T, K	293(2)	293(2)	293(2)	213(2)
ρ_{calcd}, g cm^{-3}	1.525	1.513	1.476	1.500
μ, cm^{-1}	45.40	24.54	43.96	44.67
$R_1(F_o)$, $wR_2(F_o^2)$ [$I > 2\sigma(I)$][a]	0.041, 0.057	0.039, 0.043	0.074, 0.127	0.049, 0.056
$R_1(F_o)$, $wR_2(F_o^2)$ (all data)[a]	0.114, 0.065	0.116, 0.049	0.236, 0.155	0.166, 0.067

[a] $R_1 = \sum||F_o| - |F_c||/\sum|F_o|$; $wR_2 = [\sum w(F_o^2 - F_c^2)^2/\sum w(F_o^2)^2]^{1/2}$, where $w = 1/[\sigma^2(F_o^2) + (aP)^2]$ and $P = [\max(F_o^2,0) + 2F_c^2]/3$.

seems to be compensated by the electronic stability of the *β*-**1** form. We note that simple additivity for contributions of packing and electronic energies cannot be expected: Only relative energies can be obtained by our lattice energy minimizations.

An open question concerns the apparent disagreement between the sample composition according to the powder pattern and the calculated total energies of the three phases. The *γ*-**1** form, neither favored for electronic nor for packing reasons, accounts for the same fraction as the more stable *β*-**1** modification. An explanation lies in kinetic effects because both our electronic and packing energies refer to thermodynamic equilibrium. In the case of concomitant polymorphs, kinetic effects on sample composition may become relevant at the stages of nucleation and crystal growth.

Concluding Remarks. In the present paper we had to extend the characterization of the dinuclear sandwich complex $[(C_5H_5BMe)_2Y(\mu\text{-}Cl)]_2$ in the solid state beyond conventional single crystal X-ray diffraction: The presence of the three conformational polymorphs induced us to calculate intramolecular gas-phase electronic energies and intermolecular lattice energies to evaluate the total energy differences among these modifications. A cutoff of 5−10 kJ/mol in total energy is often applied in polymorph prediction[7b,36] to avoid the generation of an intractable number of candidate structures. In the present case, the *γ*-**1** phase, for which the total energy is calculated to be more than 20 kJ/mol higher than for the most stable modification, might thus be easily overlooked.

The structural flexibility we encountered for compound **1** is an inherent characteristic of organometallic compounds.[37] For a molecule with soft internal degrees of freedom, a geometry deduced from a single X-ray structure determination should be interpreted with caution.[38] Crystallographers tend to choose a single crystal specimen from an often small or sensitive sample and do not generally ascertain that the crystalline solid consists of only a single phase. Thus, the fact that about 5% of the compounds in the CSD are know to be polymorphic[5,6] probably underestimates the real situation, and more frequent use of powder diffraction seems advisable.

Experimental Section

General Procedures. All manipulations were performed under an atmosphere of dinitrogen by means of conventional Schlenk techniques. Toluene was distilled from sodium prior to use. NMR spectra were recorded on a Varian Unity 500 (^{1}H, 500 MHz; ^{13}C, 125.7 MHz; ^{11}B, 160.4 MHz) spectrometer. Chemical shifts are given in ppm and are referenced to internal TMS for ^{1}H and ^{13}C and to external $BF_3{\cdot}Et_2O$ for ^{11}B. Mass spectra were recorded on a Finnigan MAT-95 at a nominal electron energy of 70 eV. Elemental analyses were performed at the Analytische Laboratorien, 51779 Lindlar, Germany.

Synthesis of Di-*μ*-chlorotetrakis(1-methylboratabenzene)diyttrium (1). A suspension of yttrium trichloride (489 mg, 2.51 mmol) and lithium 1-methylboratabenzene[21] (512 mg, 5.27 mmol) in toluene (20 mL) was stirred at 110 °C for 3 days. A white powder, presumed to be lithium chloride, was filtered off and washed with toluene (5 mL). The combined yellow filtrate was concentrated to ca. 5 mL. The solution so obtained was stored at 4 °C overnight to give **1** as a pale yellow moisture-sensitive crystalline solid. Crystallization of the concentrated mother liquor afforded a second crop of **1** (total yield of 650 mg, 85%).

Data for 1. ^{1}H NMR (500 MHz, C_6D_6): *δ* 7.36 (dd, $J = 10.4$, 7.0 Hz, 3-/5-H), 6.90 (dd, $J = 10.4$, 1.5 Hz, 2-/6-H), 6.26 (tt, $J = 7.0$, 1.5 Hz, 4-H), 1.13 (s, BMe). ^{13}C NMR (126 MHz, C_6D_6): *δ* 141.7 (C-3,5) 133.9 (br, C-2,6), 112.3 (C-4), 6.0 (BMe). ^{11}B NMR (160 MHz, C_6D_6, $BF_3{\cdot}Et_2O$ external): *δ* 43.2. MS (EI, 70 eV): *m*/*z* (I_{rel}) 596 (<1, $M^+ - CH_4$), 521 (75, $M^+ - C_5H_5BMe$), 430 [1, $M^+ - 2(C_5H_5BMe)$], 306 [2, $(C_5H_5BMe)_2YCl^+$], 271 [100, $(C_5H_5BMe)_2Y^+$], 215 [20, (C_5H_5BMe)-

(36) (a) Karfunkel, H. R.; Gdanitz, R. J. *J. Computat. Chem.* **1992**, *13*, 1771. (b) Gavezzotti, A. *Acc. Chem. Res.* **1994**, *27*, 309. (c) Leusen, F. J. J. *Z. Kristallogr.* **1994**, *8*, 161. (d) Gavezzotti, A. *J. Am. Chem. Soc.* **1995**, *113*, 4622. (e) Payne, R. S.; Rowe, R. C.; Roberts, R. J.; Charlton, M. H.; Docherty, R. *J. Comput. Chem.* **1999**, *20*, 262. (f) Knapman, K. *Mod. Drug Discovery* **2000**, *3*, 53.

(37) Martin, A.; Orpen, A. G. *J. Am. Chem. Soc.* **1996**, *118*, 1464.

(38) Wagner, T.; Englert, U. *Struct. Chem.* **1997**, *8*, 357.

YCl^+], 91 (40, $C_5H_5BMe^+$). Anal. Calcd for $C_{24}H_{32}B_4Cl_2Y_2$: C, 47.07; H, 5.27. Found: C, 47.01; H, 5.25.

Single Crystal Structure Determinations. Data collections were performed on ENRAF-Nonius CAD4 diffractometers equipped with graphite monochromators using the $\omega/2\theta$ scan mode. Crystal data, data collection parameters, and convergence results are listed in Table 5. The data sets of the three polymorphs were first collected at 20 °C with crystals mounted in thin-wall capillaries. Structural refinements showed that the data set of the γ-**1** form was of moderate quality. Therefore, an additional low-temperature (−60 °C) data set was collected on the same crystal. Before averaging over symmetry-related reflections, empirical absorption corrections based on azimuthal scans[39] were applied to all data sets.

The space groups of the three polymorphic phases were uniquely determined on the basis of the systemic absent conditions. The structures were solved by direct methods with the help of the SHELXS-97 program[40] and refined on reflection intensities (F^2) using the SHELXL-97 program.[41] In the final least-squares refinement all non-hydrogen atoms were assigned anisotropic displacement parameters and the hydrogen atoms were included as riding with fixed displacement parameters [C−H = 0.98 Å, U_{iso}(H) = 1.3 U_{eq}(C)].

Powder Diffraction Studies. The powder diffraction diagram was registered with a Stoe STADI2/P diffractometer equipped with a germanium monochromator (Cu Kα_1 radiation) and a position sensitive linear detector. The sample was sealed in a Lindemann capillary with 0.5 mm diameter and data were collected at room temperature.

Acknowledgment. We thank Dr. J. Huster for the powder diffraction experiment. Support of this work by the Deutsche Forschungsgemeinschaft and the Fonds der Chemischen Industrie is gratefully acknowledged.

Supporting Information Available: Tables giving detailed information on X-ray diffraction experiments as well as a synopsis of experimentally observed and calculated bond parameters, CPK representations of the molecular structures, and X-ray crystallographic files, in CIF format, for α-**1**, β-**1**, and γ-**1**. This material is available free of charge via the Internet at http://pubs.acs.org.

IC0014641

(39) North, A. C. T.; Philips, D. C. *Acta Crystallogr. A* **1968**, *24*, 351.
(40) Sheldrick, G. M. *SHELXS-97*: *Program for Structure Solution*; University of Göttingen: Göttingen, Germany, 1997.
(41) Sheldrick, G. M. *SHELXL-97*: *Program for Structure Refinement*; University of Göttingen: Göttingen, Germany, 1997.